# Analysis and Prediction of Ice Shedding for a Full-Scale Heated Tail Rotor

Richard E. Kreeger[1]

*NASA Glenn Research Center, Cleveland, OH, 44135*

Andrew Work[2]

*Ohio Aerospace Institute, Cleveland, OH, 44135*

Rebekah Douglass[3]

*Ohio Northern University, Ada, OH, 45810*

Matthew Gazella[4]

*Kent State University, Kent, OH, 44240*

Zakery Koster[5]

*Virginia Tech, Blacksburg, VA, 24060*

Jodi Turk[6]

*Cleveland State University, Cleveland, OH, 44115*

## Abstract

**When helicopters are to fly in icing conditions, it is necessary to consider the possibility of ice shed from the rotor blades. In 2013, a series of tests were conducted on a heated tail rotor at NASA Glenn's Icing Research Tunnel (IRT). The tests produced several shed events that were captured on camera. Three of these shed events were captured at a sufficiently high frame rate to obtain multiple images of the shed ice in flight that had a sufficiently long section of shed ice for analysis. Analysis of these shed events is presented and compared to an analytical Shedding Trajectory Model (STM). The STM is developed and assumes that the ice breaks off instantly as it reaches the end of the blade, while frictional and viscous forces are used as parameters to fit the STM. The trajectory of each shed is compared to that predicted by the STM, where the STM provides information of the shed group of ice as a whole. The limitations of the model's underlying assumptions are discussed in comparison to experimental shed events..**

## Nomenclature

A = cross sectional area of ice accretion
$A_P$ = cross sectional area of ice particle
ARMD = Aeronautics Research Mission Directorate
AAVP = Advanced Air Vehicles Program
b = viscous damping coefficient
B = STM viscosity term
Cd = drag coefficient
c = drag term

---

[1] Aerospace Engineer, Icing Branch, 21000 Brookpark Rd., Cleveland, OH 44135 Associate Fellow, AIAA
[2] Research Associate, Ohio Aerospace Institute, 22800 Cedar Point Rd, Cleveland, OH 44142
[3] Research Associate, Icing Branch, 21000 Brookpark Rd., AIAA Student Member
[4] Research Associate, Icing Branch, 21000 Brookpark Rd., AIAA Student Member
[5] Research Associate, Icing Branch, 21000 Brookpark Rd., AIAA Student Member
[6] Research Associate, Icing Branch, 21000 Brookpark Rd., AIAA Student Member

1

American Institute of Aeronautics and Astronautics

d = radial location of ice
F = STM friction term
Ff'= frictional force per unit length
GRC = Glenn Research Center
IRT = Icing Research Tunnel
L = length of blade
LWC = Liquid Water Content
m = mass of ice particle
MARTI = Multidisciplinary Aeronautics Research Team Initiative
MVD = Median Volume Diameter
RVLT = Revolutionary Vertical Lift Technology
STM = Shedding Trajectory Model
STAT = Shedding Trajectory Analysis Tool
t = time
$V_r$ = radial velocity
$V_t$ = tangential velocity
W = width of ice-blade contact
$\rho$ = density of ice
$\rho_a$ = density of air
$\theta$ = azimuth
$\chi_i$ = initial position of ice
$\omega$ = rotational speed

# I.   Introduction

Shedding is important to consider for rotorcraft. As ice accretes on the rotating blades, eventually aerodynamic and centrifugal forces can cause large pieces of ice to depart the rotor system. The released ice poses a ballistics danger to the aircraft as ice may impact various fuselage components, propulsion/drive system components or other blades. Additionally, shedding can occur asymmetrically and may create large vibrations due to imbalanced rotors. Accurate predictions of natural shedding and subsequent ice trajectories are critical to the definition of safe operating limits for rotorcraft not equipped with an ice protection system.

Attempts at analytically modeling ice accretion and shedding events have been performed for rotary wing aircraft, but there is still a need for further development and validation of prediction tools for ice shedding from rotorcraft blades. Ice accretion and shedding prediction can be addressed through the development of computational tools based on first-principles modeling rather than empirical methods, as well as with further collection of validation data. By developing tools to predict how and under what conditions ice accumulates along with blade shed, we can improve de-icing methods to prevent unnecessary stresses on the engine and transmission due to the imbalance caused by asymmetrical shedding and protect rotorcraft components from projectile ice. This would allow for increased overall efficiency and safety of rotorcraft. Such tools also require validation data. There are currently few methods to accurately determine the size and shape of shed ice from photos or videos of experiments, along with the ability to accurately predict trajectories of the ice particles.

These issues were investigated under a NASA Aeronautics Research Mission Directorate (ARMD) summer program in 2015 called the Multidisciplinary Aeronautics Research Team Initiative (MARTI) to address the needs of the Revolutionary Vertical Lift Technology (RVLT) Project. It was conceived with the intent to address the above gaps in technology and aid in NASA's contribution to the aerospace industry. Innovation in aerospace technology requires the knowledge and expertise in a wide variety of fields, and this is the guiding principal of MARTI. The members of this group encompassed a wide range of disciplines to achieve its goals through collaborative efforts.

This paper presents the work done by the MARTI team. It covers the development of a first-principals model made to run with NASA's LEWICE code. Additionally, it presents the data analysis methods used to obtain qualitative

American Institute of Aeronautics and Astronautics

validation from previous rotor testing in the NASA Icing Research Tunnel (IRT). This validation data is then compared to the first principles model.

## II.    Background

### 1. Overview of Shedding Models

LEWICE is a code developed by NASA for 2-D ice accretion prediction[1], and it is the core of a 3-D ice accretion tool as well. The code uses a potential panel method to determine the flow field about a clean surface, then calculates water droplet trajectories from some upstream location until they impact on the surface or until the body is bypassed. Collection efficiency is then determined from the water droplet impact location pattern between the impingement limits. A quasi-steady analysis of the control volume mass and energy balance is next performed, using a time-stepping routine. Density correlations are used to convert ice growth mass into volume. LEWICE also features multiple drop size distributions, multiple airfoil elements, thermal models for anti-icing/de-icing systems, and an interface with structured grid codes, allowing the use of viscous Navier-Stokes flow solutions.

The thermal models in LEWICE combine the features of previous codes, LEWICE/ Thermal and ANTICE, to simulate de-icing and anti-icing with electrothermal or hot air systems. Features are included to allow determination of optimized heater sequencing (for electrothermal analysis) and multiple boundary conditions (for bleed air analysis).

LEWICE has been thoroughly validated for a wide range of conditions, with a database of over 3,000 ice shapes on 9 different geometries. The validation database lies mostly within the Federal Aviation Administration's icing certification criteria 14 CFD Part 125, Appendix C continuous maximum or intermittent maximum envelopes, and there are some exceedence and super-cooled large droplet conditions for comparison as well. This validation, along with significant research into recommended test methods and advanced component models, has led to a degree of acceptance of LEWICE for use in reducing the cost of development and certification programs for fixed-wing applications. However, this level of acceptance has not yet been achieved for rotary-wing applications.

The LEWICE code is able to simulate rotor blade ice accretions, but at a much lower level of fidelity than for fixed-wing aircraft. In part this is due to the assumptions made about the underlying physics. The software allows inputs for rotational speed to calculate an increase in the aerodynamic heating term in the energy balance.

LEWICE does not simulate a fully rotational system, but does allow the user to input a number of simple parameters- distance from the hub to the 2-D section of interest, rotation speed, and orientation of the plane of rotation (vertical for propellers, horizontal for rotors). The rotational force is used to determine ice shedding and to find the resultant force of the shed ice particle, which is used to track the particle after it sheds. The rotational speed is also used to calculate an increase in the aerodynamic heating term in the energy balance. But the rotating body information is not used by the potential flow solver in LEWICE, nor is the rotating body information used by the trajectory equation.

Higher fidelity self-shedding analyses[2,3] have also been developed and demonstrated for rotorcraft. These are typically based on empirical adhesion models expanding on the methods of Fortin et. al.[4] and Flemming et. al.[5] These simulations involve using a computational fluid dynamics code like OVERFLOW coupled to the ice accretion code LEWICE. In cases where the rotor is not sufficiently rigid, these approaches also loosely couple to a computational structural dynamics code such as DYMORE. After each update of the ice shape, tools based on these methods compare the centrifugal forces outboard of a given radial station to the adhesion and cohesion forces expected at each cross section of the ice shape. The surface shear stresses are based on temperature and surface material, using empirical curves. From this analysis, the time of shed, thickness and length of the shed ice shape can then be predicted. The shed location and time are reasonably well predicted using these methods.

The adhesion force (in Pascals) model used by LEWICE is defined by empirical equations based on Reich and Scavuzzo[6]. Note that this model uses temperature as the only parameter, and is based on a limited set of material properties with a high degree of scatter.

One difficulty in moving to a physics-based prediction of adhesion strength is that current predictive models of ice adhesion strength are really only valid on the micro scale (nanometer) range. These small-scale models evaluate

3

adhesion strength by calculating the energy of van der Waals forces. Current macro-scale models use temperature as the only parameter, and are based on a limited set of material properties with a high degree of scatter. An improved prediction of ice adhesion- and hence, shedding in some cases- must account for the macro scale (micrometer) range effects of ice expanding into surface roughness elements. Progress has been made towards developing a model to predict adhesion strength using key parameters related to macro-scale effects[7,8,9] but further work is necessary to explore the model capability for more complicated, realistic surfaces.

## 2. Experimental Setup

In August and September of 2013, researchers from Bell, Boeing, Sikorsky, Georgia Tech and NASA Glenn conducted rotor blade icing tests in the IRT.[10,11,12] The rotor model test had multiple objectives, including ice accretion, ice shedding trajectory and impact, deice and anti-ice system performance, and rotor performance. High quality data for rotor blade icing was obtained. Data included rotor ice shapes, rotor performance, deice and anti-ice performance with runback/refreeze, shed ice trajectories and impact data. Ice shapes were documented by laser scan, hand tracing and photograph.

The IRT is a closed-loop refrigerated wind tunnel able to attain velocities up to 350m.p.h. The test section is 6ft. high, 9ft. wide and 20ft. long. The total air temperature in the test section can be varied from -20° F to +33° F. A system of spray bars generates a cloud of super-cooled liquid droplets with a liquid water content (LWC) between 0.2 and 3.0 grams/m$^3$ and a median volume diameter (MVD) of drops between 14 to 50 μm at Appendix C conditions.

The tested rotor system was a two bladed teetering tail rotor with heater blankets bonded to the blade surface. The 65 inch diameter rotor was tested to 150 knots forward airspeed. The blades were 5.25-inch chord as shown in Figure 1. Blade pitch and rotation speed (RPM) were controlled by the model operator. Although the model was not equipped with cyclic control, the rotor and drive systems were designed to permit changes in the (fore/aft) rotor mast angle up to +/- 10 degrees. The rotor tip speed was representative of a full scale main rotor tip in forward flight.

High-speed Phantom cameras were placed in the IRT to capture shed events. One camera was placed in the ceiling, covered by a transparent guard, and about fifteen degrees offset from perpendicular to the ceiling. The overhead view from this camera captured half of the rotor blade's rotation and the thin aluminum panels that shielded the side windows of the IRT as shown in Figure 2. These aluminum panels were also set with the same mast-tilt as the rotor blades. Several variables changed from test run to test run in the IRT. A few such variables included the rotor speed, wind speed, various heating schemes, and attack angles of the rotor blades. After test runs that did not have sheds, the ice was painted, scanned, and hand sketches were taken at various radii down the rotor blade. Two of the test runs contained a total of three shed events which were captured at a sufficiently high frame rate to obtain multiple images of the shed ice in flight.

American Institute of Aeronautics and Astronautics

**Figure 1. Rotor model in the Icing Research Tunnel**.
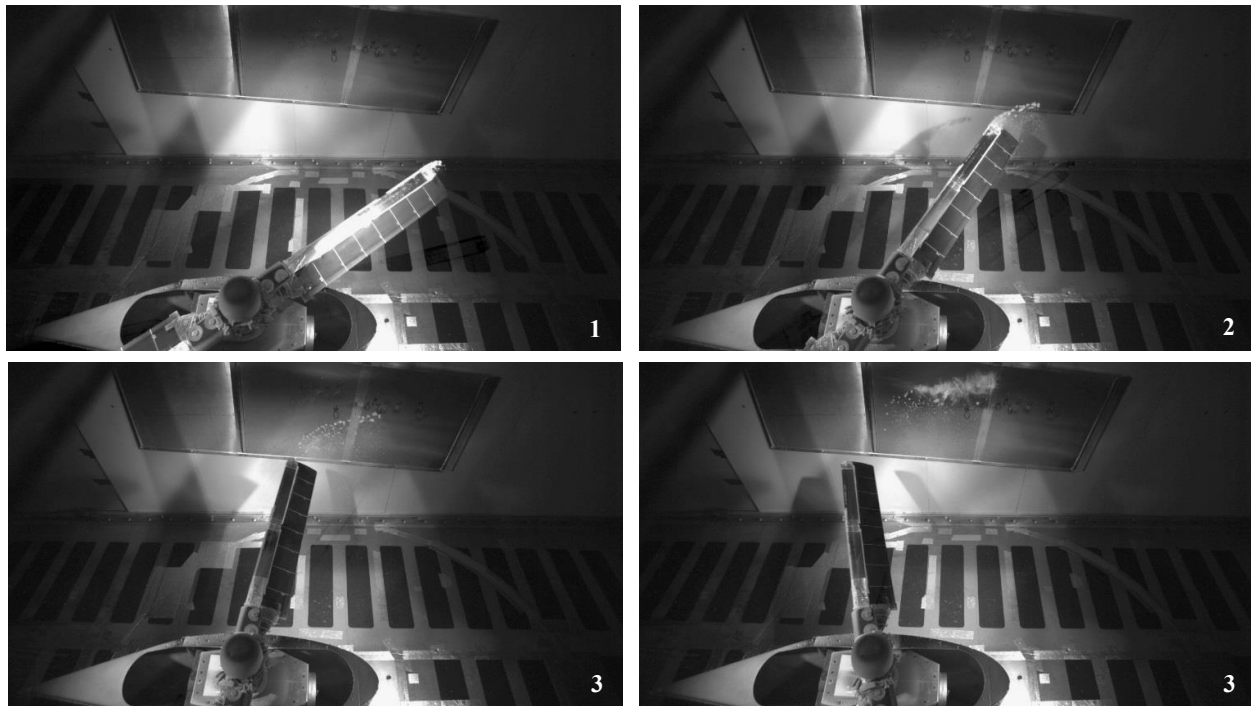


**Figure 2. Run 67 Shed Event (View from Top Camera).**

American Institute of Aeronautics and Astronautics

# III.    Data Analysis

In this section, the analysis of the three shed events from previous testing will be presented and compared to an analytical model. Videos of the heated rotor experiment from a high speed camera within the IRT were analyzed, and this data was converted into perspective-corrected images of a shed event through a process which will be described below. From these corrected images, useful data on the shed ice particles were obtained, in particular the position of the particle centroids, which allowed the velocity and acceleration to be calculated for individual particles. The Shedding Trajectory Analysis Tool (STAT) was developed to automatically process the images and allow the experimental trajectory data to be overlaid with predictive model results for comparison. The predictive model, the Shedding Trajectory Model (STM), was created to predict the ice shed, which was fit to the data through physical parameters.

## 1. Image Processing and Shedding Trajectory Analysis Tool

In this section, the general methodology used to perform image processing will be described. Of the two cameras used to capture shedding events, the ceiling camera videos were selected for analysis since the tunnel camera showed that ice at the leading edge of the cloud stayed roughly in the plane of the rotor disc, but were otherwise not amenable to analysis. Videos recorded were not triggered and contained a large number of images. To isolate shed events, the total image intensity was calculated excluding the region of the image containing the rotor disc. Using this method, shed events showed up as peaks. Shed events were identified by thresholding the total intensity of all of the images by the average total intensity Once the images that capture a shed event were extracted from the Phantom videos, they had to be processed to acquire meaningful quantitative data about the shed characteristics. A MATLAB code was developed to perform a variety of tasks centering on the analysis of the shed trajectories. This code is termed the Shedding Trajectory Analysis Tool (STAT); an overview for this code is shown in Figure 3.

The second task performed by the STAT was to transform the shed images into binary images isolating ice particles, so that their sizes, velocities, and kinetic energies could be approximated. Prior to conversion, the image had perspective distortion due to the placement of the camera. This prohibited the direct measurement of parameters such as particle location and area. A four-point projective plane transformation was used to correct perspective distortion. Points were selected in the rotor plane by isolating a feature on a given rotor and obtaining its coordinates in multiple images. Frames were selected to give the widest available distribution of coordinates to minimize error during the transformation. Extra points were identified in order to verify the accuracy of the transformation, where the points were visually determined to fall within three pixels of a circle encompassing the rotor disc. The transformation is only valid for points laying inside (or close to) the plane of the rotor disc, and so detailed analysis for particles off of the leading edge of the shed ice cloud was not performed. Corrected images had a resolution of 10 pixels per inch in the plane of the rotor disk. Using this ratio, valuable data such as trajectories and velocities were calculated directly. Particle areas were also calculated which allowed the mass to be estimated. Using the estimated mass and calculated acceleration of the particles, the drag force and coefficient of drag on each particle were estimated.

Images were then background subtracted by creating a median image of all images used for analysis (5-7 images), and subtracting this median image from each image. This allowed for ice and the rotor to be isolated in each image. The rotor disc was excluded from further analysis. The images were converted to binary format by performing an Otsu threshold. At this point, the centroid and pixel area of each particle was calculated and the mass estimated.

American Institute of Aeronautics and Astronautics
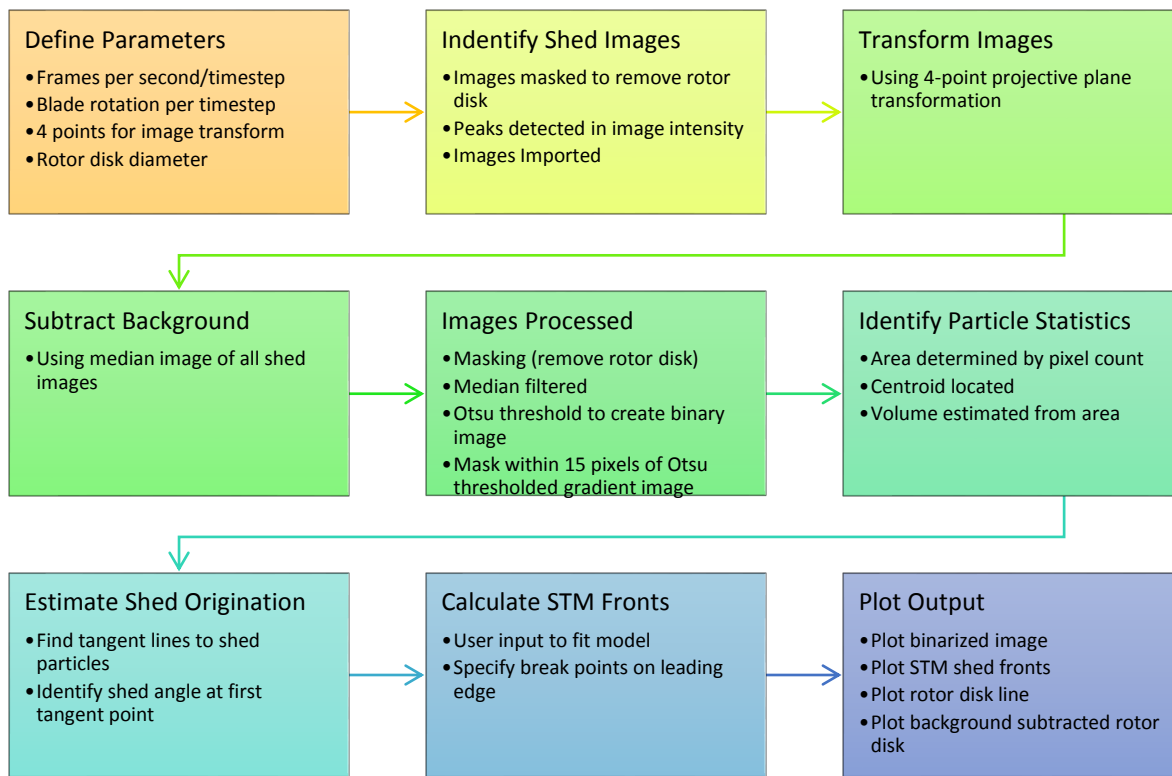
**Figure 3. Flowchart of the STAT script.**

The STAT tool is a MATLAB script which was created to perform the image processing and to overlay and fit the model to test data. The work flow was set up such that the leading edge of the ice was plotted for each time step used for analysis. Multiple breaks in the ice were visually identified and lengths were measured to feed into the model. Each break was color-coded to keep them separate. Three shed events provided sufficiently large ice sheds to analyze and also were recorded at a high enough frame rate, listed in Table 1. Two sheds were present in Run 67, and one was present in run 71. Run 71 was particularly interesting since it contained three breaks in the ice.

| | Description | Rotor Speed (rpm) | Blade Pitch (deg) | Tunnel Static Temperature ($^o$F) | Tunnel Speed (kts) | LWC (g/m$^3$) | MVD μm |
|---|---|---|---|---|---|---|---|
| **Run 67** | Chordwise De-ice | 1200 | 10 | -4 | 60 | 0.5 | 15 |
| **Run71** | Spanwise De-ice | 1200 | 5 | -4 | 60 | 0.5 | 15 |

**Table 1. Usable Shedding Run Matrix.**

## 2. Shed Ice Characterization

After the image has been successfully converted to binary using these methods, the STAT was used to create a table of all the detected particle pixel areas and centroid locations. A histogram of the particle size distribution was created by the code and the table of area and centroid data can be saved in a spreadsheet. The centroids can be plotted on top of a complement image for reference.

American Institute of Aeronautics and Astronautics

The distribution of particle masses was found to be a non-normal distribution, which is common for ice shatter. The particle size distribution histogram showed hundreds of small, snowy particles, several medium-sized ones, and a few larger (~1-2 inches in visible area) particles. The larger particles are the ones mainly of concern when with regards to impact danger. The particle mass distribution for three runs is shown in Figure 4. Run 83, a natural shed, was excluded due to the length of the shed ice being insufficient for reasonable comparison.

Since the particles have complex geometries, it was decided to approximate them as spheres since no out-of-plane information was available. Such a model was believed to overestimate the size of the particles, which was desirable to obtain a conservative estimate of the potential damage of the ice. Based on the spherical assumption important parameters such as equivalent diameter, volume, and mass were obtained.
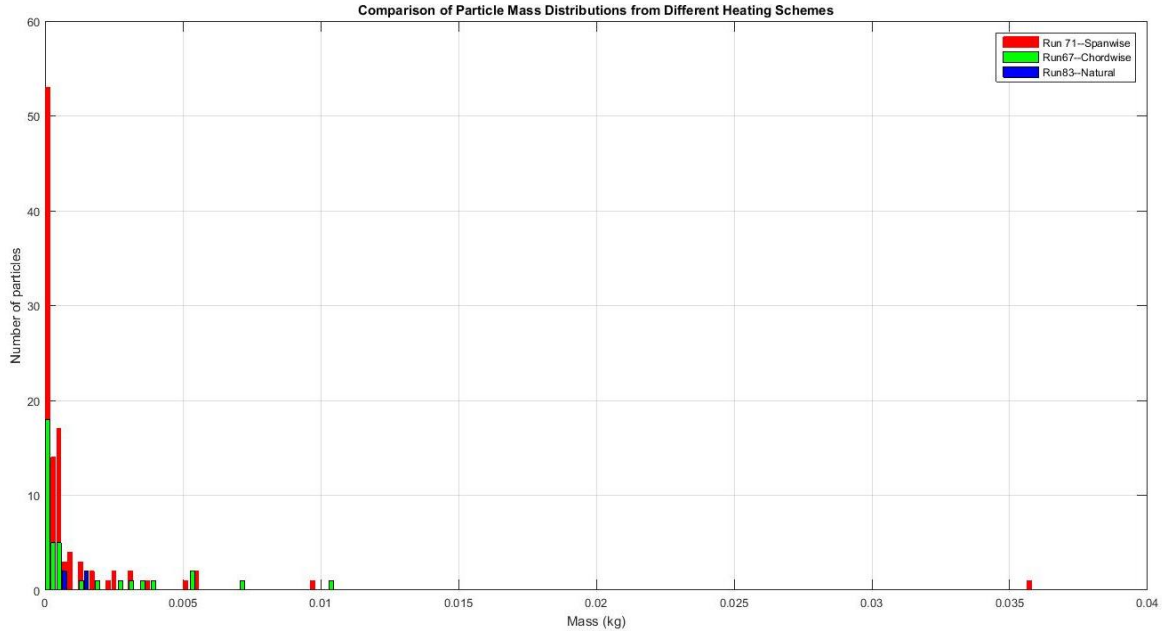


**Figure 4. Combined histogram of calculated particle mass distributions for three shed events.**

### 2. Development of Predictive Model

The STM was developed to predict the location of the shed ice during a shed event. The STAT tool processes raw data and overlays the STM prediction onto the black and white shed images, allowing the predicted shed front to be compared to acquired test data. The tool uses the time since shed, the rotor position at shed onset, and the boundary locations of the shed ice on the blade as inputs. The STM can handle continuous ice sheds at any point on the blade, so that multiple breaks can be accommodated.

The movement of ice during a shed event is described in two stages, the first while the ice is on the rotor edge, and the second after it has left the rotor edge. In the first stage, it was assumed that the rotor front edge line intersected the center of the rotor disk, and rotated in a 2D plane with constant velocity. The front edge line of the rotor blade did not intersect the center of the rotor disk and was offset by approximately 1.5 inches. The second stage was assumed to be a 2D ballistics problem with quadratic drag, where the ice broke instantly as it passed the tip of the rotor. To maintain simplicity, drag from the flow of the tunnel was not included. Figure 4 shows the coordinate system used for this problem. The ice break starts at d1 and ends at d2, while the length of the blade (L, not shown) may exceed d2. The X axis rotates with the rotor blade.

The position during the second stage was calculated as follows. The initial position was determined

$$x_i = L\cos(\omega t + \theta_i)\,\hat{\imath} + L\sin(\omega t + \theta_i)\,\hat{\jmath}$$

8

where $\omega$ was the rotational speed of the rotor in rad/s, $L$ was the length of the rotor blade in inches, and $\theta_i$ was the angle when the ice reached the end of the blade, which was the angle the shed began at in the case that the ice began at the edge. The tangential velocity was calculated

$$V_t = \omega L$$

and the radial velocity, $V_r$, was determined from the first stage. This allowed the initial velocity to be calculated

$$V_i = (V_r \cos(\omega t + \theta_i) - V_t \sin(\omega t + \theta_i))\hat{\imath} + (V_r \sin(\omega t + \theta_i) + V_t \cos(\omega t + \theta_i))\hat{\jmath}$$

Assuming a constant coefficient of drag, the position was then calculated

$$x_2(t) = \frac{m}{c} \ln\left(1 + \frac{cV_i t}{m}\right)$$

where $c = \frac{c_d A_p \rho_a}{2m}$, $c_d$ is the coefficient of drag, $\rho_a$ is the density of the air, $A_p$ is the cross sectional area of a particle, and m is the mass of a particle. The position function was fit for the entire shed (not individual particles) by varying $c$ as a single term.
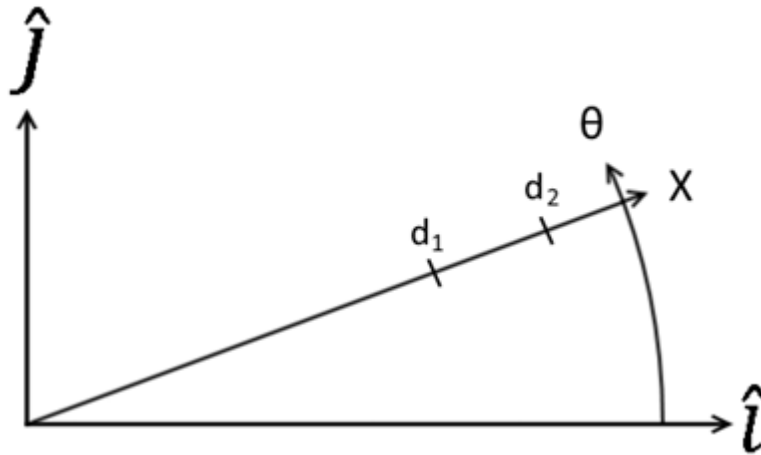


**Figure 5. The coordinate system for the STM.**

The motion of the ice during the first stage was needed to obtain the radial velocity in the second stage. The derivation for the position of the ice in the first stage is as follows. The position along the blade relative to the rotor hub was $x_s$. The first stage occurred in two parts (if $d_2 < L$). In the first part, the ice slides as one solid piece until it reaches the blade tip. In the second, the ice continues to slide but is broken off as it passes the tip. The point separating these two parts is when the ice reaches the tip,

$$z = L + d_1 - d_2$$

The force on the ice mass has two terms, that due to centripetal acceleration (1ˢᵗ term), and resistive forces (viscous drag while sliding across a liquid layer or friction if poorly lubricated).

9

$$F_i(x_s) = \begin{cases} \dfrac{\rho A \omega^2}{2}(2x_s(d_2 - d_1) + (d_2 - d_1)^2) - (d_2 - d_1)(\dot{x}_s bW + F_f'), x_s < z \\ \dfrac{\rho A \omega^2}{2}(L^2 - x_s^2) - (L - x_s)(\dot{x}_s bW + F_f'), x_s \geq z \end{cases}$$

where $\rho$ is the density of the ice, $A$ is the cross sectional area of the ice (assumed constant along the length of the rotor blade), b is the viscous damping coefficient, W is the width of the ice-blade contact area (along the thickness of the blade), and $F_f'$ is the frictional force per unit length. The mass was calculated

$$M_i(x_s) = \begin{cases} \rho A(d_2 - d_1), x_s < L + d_1 - d_2 \\ \rho A(L - x_s), x_s \geq L + d_1 - d_2 \end{cases}$$

and the acceleration was calculated

$$a_i(x_s) = \frac{F_i(x_s)}{M_i(x_s)} = \begin{cases} \dfrac{\omega^2}{2}(2x_s + (d_2 - d_1)) - \dfrac{(\dot{x}_s bW + F_f')}{\rho A}, x_s < z \\ \dfrac{\omega^2}{2}(L + x_s) - \dfrac{(\dot{x}_s bW + F_f')}{\rho A}, x_s \geq z \end{cases}$$

At this point it is helpful to make two substitutions, and put the acceleration equation into differential form:

$$B = \frac{bW}{\rho A}$$

$$F = \frac{F_f'}{\rho A \omega^2}$$

$$\begin{cases} \ddot{x}_s + B\dot{x}_s - \omega^2 x_s = \dfrac{w^2(d_2 - d_1 - 2F)}{2}, x_s < z \\ \ddot{x}_s + B\dot{x}_s - \dfrac{\omega^2}{2}x_s = \dfrac{w^2(L - 2F)}{2}, x_s \geq z \end{cases}$$

The differential equations have the particular solution:

$$x_p(t) = \begin{cases} F - \dfrac{d_2 - d_1}{2}, x_s < z \\ 2F - L, x_s \geq z \end{cases}$$

The characteristic equations for the differential equation were used to solve the complementary solution, and are as follows:

$$\begin{cases} r^2 + Br - \omega^2 = 0, x_s < z \\ r^2 + Br - \dfrac{\omega^2}{2} = 0, x_s \geq z \end{cases}$$

where the roots are

$$r_{1,2} = \frac{\left(-B \pm \sqrt{B^2 + 4\omega^2}\right)}{2}$$

$$r_{3,4} = \frac{\left(-B \pm \sqrt{B^2 + 2\omega^2}\right)}{2}$$

10

American Institute of Aeronautics and Astronautics

The complementary solution takes the form

$$x_c(t) = \begin{cases} c_1 e^{r_1 t} + c_2 e^{r_2 t}, x_s < z \\ c_3 e^{r_3 t} + c_4 e^{r_4 t}, x_s \geq z \end{cases}$$

and combined with the particular solution, gives the function for the position of the ice along the rotor

$$x_s(t) = \begin{cases} c_1 e^{r_1 t} + c_2 e^{r_2 t} + F - \dfrac{d_2 - d_1}{2}, x_s < z \\ c_3 e^{r_3 t} + c_4 e^{r_4 t} + 2F - L, x_s \geq z \end{cases}$$

The velocity of the ice along the rotor is the derivative of the position function,

$$\dot{x}_s(t) = \begin{cases} c_1 r_1 e^{r_1 t} + c_2 r_2 e^{r_2 t}, x_s < z \\ c_3 r_3 e^{r_3 t} + c_4 r_4 e^{r_4 t}, x_s \geq z \end{cases}$$

The coefficients are solved using the following initial conditions

$$x_s(0) = \begin{cases} d_1, x_s < z \\ z, x_s \geq z \end{cases} \qquad \dot{x}_s = \begin{cases} 0, x_s < z \\ V_{1f}, x_s \geq z \end{cases}$$

where $V_{1f}$ is the velocity at $x_s = z$ from the first part. The coefficients are as follows:

$$c_1 = \frac{d_1 + d_2 - 2F}{2\left(1 - \dfrac{r_1}{r_2}\right)}$$

$$c_2 = \frac{d_1 + d_2 - 2F}{2\left(1 - \dfrac{r_2}{r_1}\right)}$$

$$c_3 = \frac{V_{1f} - r_4(2L - 2F - d_2 + d_1)}{r_3 - r_4}$$

$$c_4 = \frac{V_{1f} - r_3(2L - 2F - d_2 + d_1)}{r_4 - r_3}$$

The radial velocity was then obtained for a given time after initial shed using $\dot{x}_s(t)$.

This model provided four terms to fit the model to the data: $\theta_i$, $B$, $F$, and $c$; alternatively the substitution terms B and F can be used directly for viscosity and friction. The first was set to match the position of the blade when the ice initially broke. The friction and damping terms were varied to match the position of the ice as it slid along the blade, and the drag term was set to match the position of the ice in stage 2.

### IV.     Results and Discussion

The STM was programed into the STAT, allowing the model to be fit to captured shed events. The following results are provided by the STAT tool, and show the necessity and applicability of using the fit parameters. Figure 5 shows the ice shed on Run 71 compared to the idealized model. The gray circle represents the rotor disk, inside the circle are images of the rotor blade at each time step. Outside the circle in white is the detected ice. The yellow lines are idealized trajectory lines tangent to the rotor disk (no radial velocity). The green, red, and blue lines are the model position for each of the three breaks.
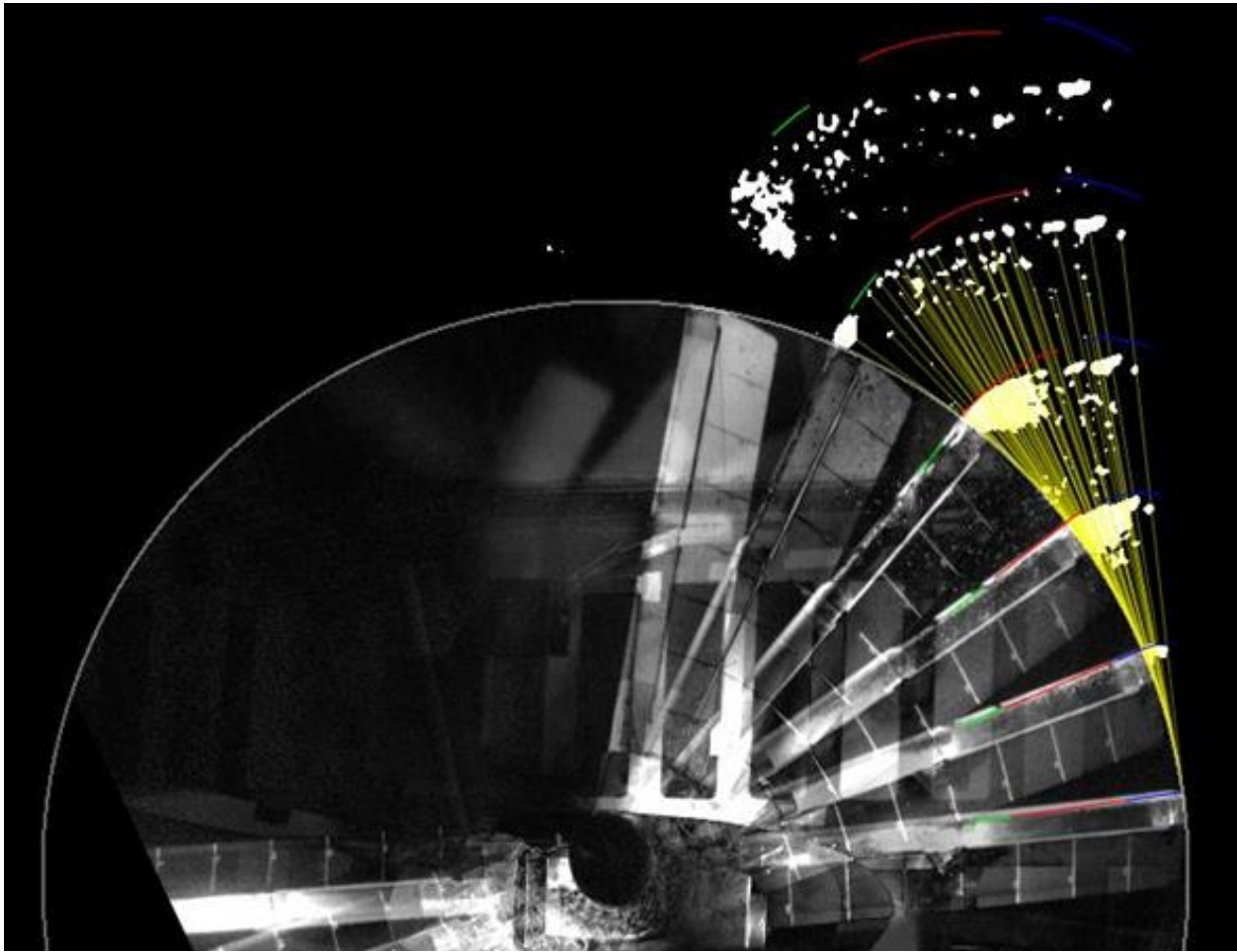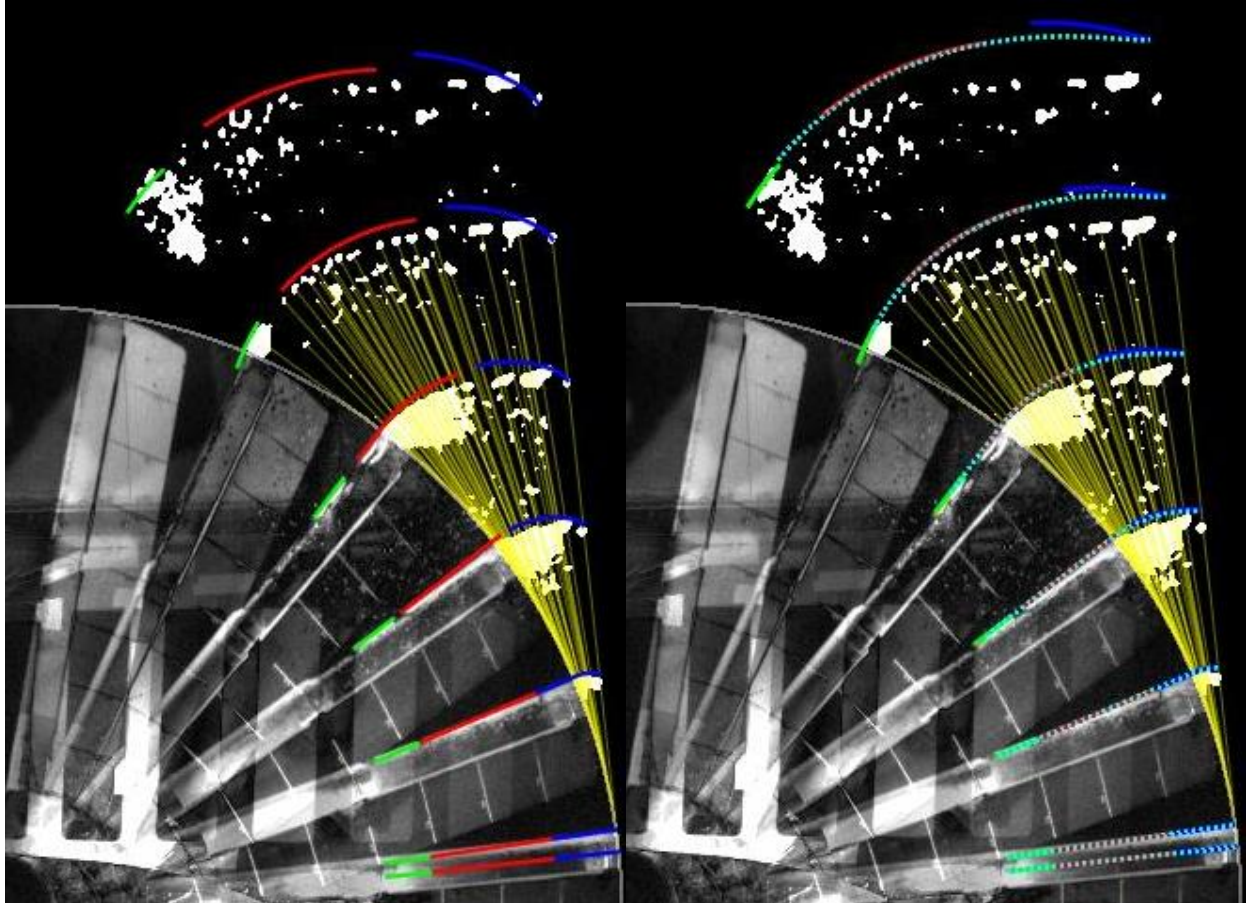
**Figure 6. Shed Ice Position Compared to unmodified STM, Run 71. F = 0, B = 60, c = 0.0004, θ = 0.**

The STM over-predicted the radial velocity of the ice off the rotor since it assumed the ice accelerated freely along the edge of the rotor blade, and didn't account for drag on the particles in the air. This is particularly obvious when investigating the third piece of ice sliding off the edge of the rotor, which the STM attempted to predict with the green line. The STM far outstrips the ice before it exits the rotor blade. It can also be seen that the predicted shed fronts pull away from the actual ice with increasing spacing at each time step. To correct for this, the STM was updated to include friction and damping terms while the ice was on the blade, and a drag term while the ice was off the blade. The STM was then fit to the data by adjusting these parameters, the result of which is shown in Figure 6.

As seen in Figures 5 and 6, Run 71 was a special case with three breaks. This allowed for a very close match when fitting the STM since friction and damping while on the blade could be adjusted to match the position of the ice while it was on and off the blade. Increasing damping tended to provide longer fronts by slowing the ice very little at the start of the shed, but slowing it greatly as the last of the ice neared the tip when radial velocity reached a maximum. Friction tended to slow the group more at the beginning of the shed, and resulted in shorter shed fronts overall. It was not possible to match the results perfectly which indicates that the physics of the problem are more complicated than the STM assumes.

Drag due to the wind tunnel flow was not included and might be required for a better fit. Some error is also attributable to the ice not breaking continuously as it sheds, particularly in the first group off the edge of the blade. To

12

American Institute of Aeronautics and Astronautics

identify each term used to fit the STM with a reasonable degree of certainty, more data from future experimental tests would be required. The present analysis is meant to show that the STM is capable of fitting the data, and providing a reasonable estimate of the velocity distribution of a shed event, and can fit the length of multiple breaks in a single shed event.



**Figure 7. Shed Ice Position Compared to Fit STM, Run 71. Left: F = 0, B = 60, c = 0.0004, θ = 0. Right: F = 0, B = 60, c = 0, θ = 0, dotted cyan line is predicted front with no interstitial breaks.**

Run 71 was also compared to a case where no interstitial breaks were calculated. This is shown on the right side of Fig. 6, where the dotted cyan line represents the shed front of a solid piece of ice of the same size as all three pieces on the left. When the interstitial breaks are ignored, the shape has several predictable changes. First, the ice at the front of the group is slowed by the ice closer to the center of the rotor since that ice experiences smaller centrifugal forces, and expanded to bridge the gap between groups. The second group (red) is only expanded, since the gain and loss from the first and third groups nearly balance out. The third group is dragged off of the rotor blade much more quickly, resulting in a smaller fan angle. The total front area is increased compared to a shape with multiple breaks. These differences highlight the shortcoming of assuming the ice breaks continually as it leaves the edge of the rotor.

13

American Institute of Aeronautics and Astronautics
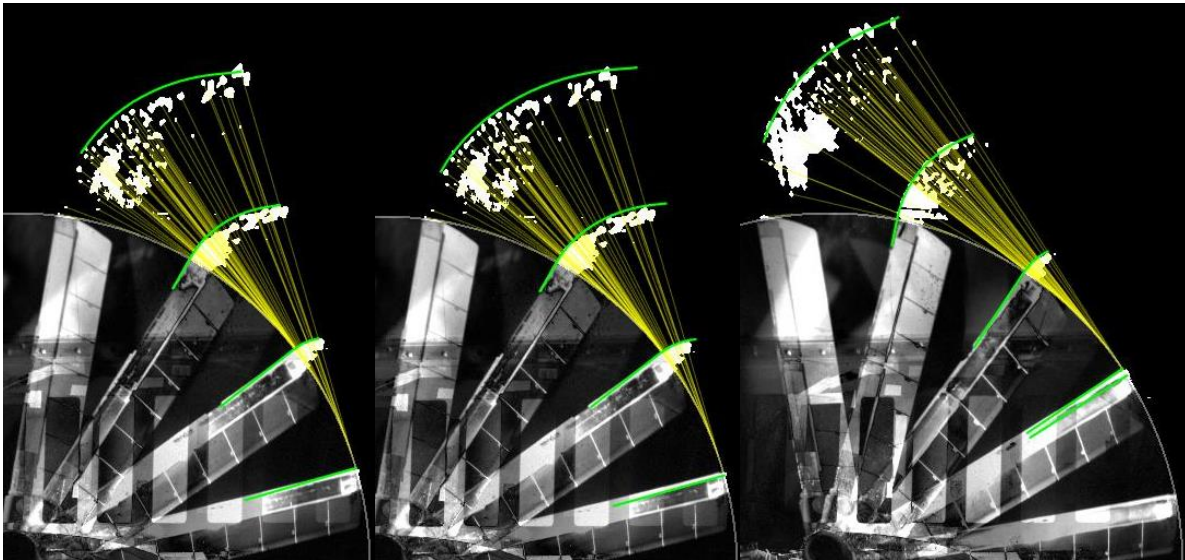
**Figure 8. Shed Ice Position Compared to Fit STM, Run 67. Left: Shed 1, F = 0, B = 60, c = 0, θ = 0. Middle: Shed 1, F = 0, B = 140, c = 0, θ = 4. Right: Shed 2, F = 0, B = 60, c = 0, θ = 0.**

The drag term was set to zero for Figure 8 to show the predicted front progressively moving ahead of the actual front, which was not noticeable in Run 67 as it was in Run 71. Two shed events from Run 67 were also fit, and are shown in Fig. 7. The viscous term was varied for Shed 1 in Run 67 from 60 to 140, showing the lengthening of the shed front with increasing drag. The variation of other parameters did not give a better fit to the data. In general, the viscous term was found to have more of an effect on the end of the shed front than the beginning since it resisted the sliding of the ice more as the relative velocity between the ice and the blade increased. The friction term did not possess this effect, and by varying both the position of the ice while on and off the blade, could be matched closely. Shed 2 from Run 67 shows the ice moving ahead of the shed front, even though drag was set to zero in the STM. It is speculated that this may be error due to ice rising above the rotor plane, where the perspective transformation becomes invalid. This was likely caused by vibration in the test stand due to the imbalance created from Shed 1. Conversely, the predicted shed front in Shed 1 appears to move ahead of the ice. This is suspected to be the case since the particles should be slowing down from drag forces. As evidenced by these two opposite conditions, the quality of the data is such that fine tuning of the drag term cannot be performed – again indicating that more data is needed for a proper fit.

This research developed a promising method of modeling ice shedding trajectories. The dynamics and effects of ice shedding on rotary blades were analyzed using a Shedding Trajectory Analysis Tool, and new methods for investigating the physics of shed events and the consequences they have on rotorcraft were developed. This method of data analysis and additional reduced data can be used to further validate the analytical Shedding Trajectory Model developed herein. This set of tools that comprise a possible first step for a future code that will work together with LEWICE to more accurately model the shed of ice in a variety of air vehicle applications, enabling safer, more efficient ice protection systems.

14

American Institute of Aeronautics and Astronautics

# References

[1] Wright, W., "User's Manual for LEWICE Version 3.2," NASA/CR-2008-214255, November, 2008.

[2] Bain, J., Cajigas, J., Sankar, L., Flemming, R., and Aubert, R., "Prediction of Rotor Blade Ice Shedding using Empirical Methods," AIAA 2010-7985, AIAA Atmospheric and Space Environments Conference, Toronto, Canada, 2-6 August, 2010.

[3] Kim, J., Sankar, L., Palacios, J., and Kreeger, R., "Numerical and Experimental Studies of Rotorcraft Icing Phenomena," American Helicopter Society European Rotorcraft Forum, 2015.

[4] Flemming, R.J. and Lednicer, D.A., "High Speed Ice Accretion on Rotorcraft Airfoils," NASA CR-3910, November 1984.

[5] Fortin, G and Perron, J., "Spinning Rotor Blade Tests in Icing Wind Tunnel," AIAA Paper 2009-4260.

[6] Scavuzzo, R.J., Chu, M.L., and Kellackey, C.J.; "Impact Ice Stresses in Rotating Airfoils." AIAA-90-0198, 28th Aerospace Sciences Meeting, January 8-11, 1990, Reno, Nevada.

[7] Brouwers, E., Palacios, J., Smith, E., and Peterson, A., "The Experimental Investigation of a Rotor Hover Icing Model with Shedding," American Helicopter Society 66th Annual Forum, Phoenix, AZ, 11-13 May, 2010.

[8] Knuth, T., Palacios, J., Wolfe, D., Kreeger, R., Smith, J., Wohl, C., and Palmieri, F., "Ice Adhesion Strength Modeling Based on Surface Morphology Variations," presented at the SAE 2015 International Conference on Icing of Aircraft, Engines and Structures, Prague, the Czech Republic, 22-25 June, 2015.

[9] Kreeger, R., Sankar, L., Narducci, R., and Kunz, R., "Progress in Rotorcraft Icing Computational Tool Development," SAE Technical Paper 2015-01-2088

[10] Wright, J., and Aubert, R., "Icing Wind Tunnel Test of a Full Scale Heated Tail Rotor Model," presented at the AHS 70th Annual Forum, Montreal, Canada, 20-22 May, 2014.

[11] Narducci, R., Wright, J., and Aubert, R., "Rotor Performance of a Full-Scale Heated Tail Rotor," presented at the American Helicopter Society 71st Annual Forum, Virginia Beach, Virginia, 5-7 May, 2015.

[12] Kreeger, R., and Tsao, J., "Ice Shapes on a Tail Rotor," presented at the AIAA 6th Atmospheric and Space Environments Conference, Atlanta, GA, 16-20 June, 2014.

American Institute of Aeronautics and Astronautics